IEEE Photonics Journal
An IEEE Photonics Society Publication

Open Access

Lumped Dissipation Induced Quasi-Phase Matching for Broad and Flat Optical Parametric Processes

Volume 11, Number 6, December 2019

Hanwen Hu
Lei Zhang
Chi Zhang
Yuntian Chen
Jing Xu
Xinliang Zhang

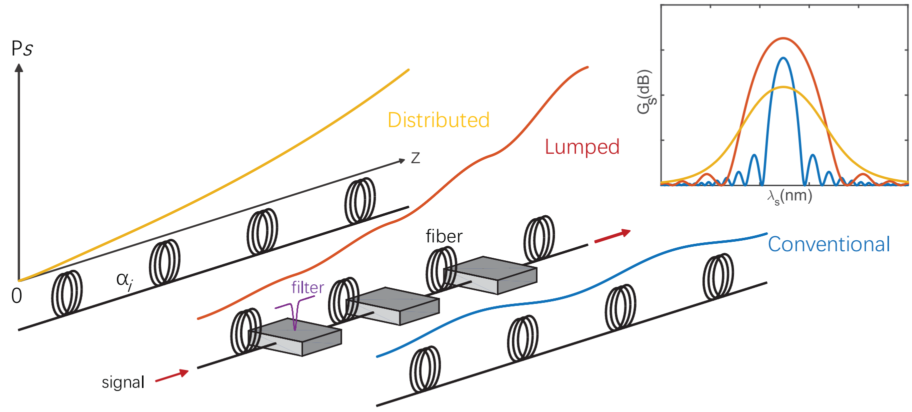

DOI: 10.1109/JPHOT.2019.2947331

Lumped Dissipation Induced Quasi-Phase Matching for Broad and Flat Optical Parametric Processes

Hanwen Hu,[1] **Lei Zhang**,[2] **Chi Zhang**,[2] **Yuntian Chen,**[1,2] **Jing Xu**,[1,2] **and Xinliang Zhang** [1,2]

[1]School of Optical and Electronic Information, Huazhong University of Science and Technology, Wuhan 430074 China
[2]Wuhan National Laboratory for Optoelectronics, Huazhong University of Science and Technology, Wuhan 430074 China

DOI:10.1109/JPHOT.2019.2947331

Manuscript received August 30, 2019; revised September 29, 2019; accepted October 8, 2019. Date of publication October 14, 2019; date of current version November 26, 2019. This work was supported in part by the National Natural Science Foundation of China under Grants 61775063 and 61735006, in part by the National Key Research and Development Program of China under Grant 2017YFA0305200, and in part by the Fundamental Research Funds for the Central Universities, HUST, under Grant 2018KFYYXJJ055. *(Hanwen Hu and Lei Zhang contributed equally to this paper.)* Corresponding authors: Chi Zhang; Jing Xu (e-mail: chizheung@hust.edu.cn; jing_xu@hust.edu.cn).

Abstract: Distributed dissipation in optical parametric processes has attracted renewed interests recently due to its rich physics including modulation instability, gain broadening, unidirectional energy transfer etc. Due to difficulties in practical implementation, lumped dissipation are investigated in this work as an alternative approach which can be realized more conveniently. Strong similarities are found between lumped and distributed dissipation. While distributed losses contribute to non-hermitian phase matching, lumped dissipation is shown to be a simple and universal quasi-phase matching method. Experimental validations of gain broadening and flattening in normal and anomalous dispersion regions are presented. As an application to wavelength conversion, enlarged conversion bandwidth when dissipation is introduced to the signal wave is revealed.

Index Terms: Optical signal processing, fiber nonlinear optics.

1. Introduction

The idea of harvesting gain through dissipation in optical parametric processes has attracted renewed interests recently [1]–[6] due to its rich physics including modulation instability in normal dispersion regime [1], optical parametric amplification (OPA) enabled by non-hermitian phase matching [2], high conversion efficiency in chirped pulse amplification [3], related applications to optical parametric oscillation [7] and optical frequency comb generation [4] etc. However, distributed losses are in general difficult to implement and have been so far demonstrated using stimulated Brillouin scattering (SBS) [1] or appropriate material with required loss dispersion [3]. On the other hand, lumped dissipation may offer a viable alternative to distributed dissipation, which can be simply realized using a series of optical filters. Gain enhancement based on lumped attenuation between two sections of fibers has been reported [8]. However, such work focuses on the pump depletion regime and no comprehensive theory has been proposed. In this work, we theoretically and experimentally investigate the impact of lumped dissipation on optical parametric processes based on third-order nonlinearity, as shown in Fig. 1(a) where the idler wave is attenuated to be

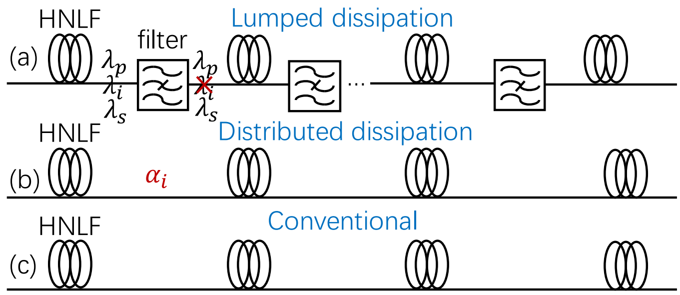

Fig. 1. Schematic diagram of three different OPA scenarios: (a) lumped dissipation is introduced to the idler wave, (b) distributed dissipation α_i is introduced to the idler wave, (c) conventional OPA. Transmission losses of all waves are not taken into account. OPA: optical parametric amplification; HNLF: highly nonlinear fiber.

much smaller than the signal wave after filtering. OPA with distributed losses α_i introduced to the idler wave is shown in Fig. 1(b) and conventional OPA is shown in Fig. 1(c). Special focus is given to the comparison between lumped and distributed dissipation with the assistance of analytical formulations. While distributed losses contribute to non-hermitian phase matching [2], it will be shown that the role of lumped dissipation is to provide quasi-phase matching (QPM). Note that various schemes of QPM in case of third order OPA have been reported, such as rearranging the nonlinear media [9], dispersion compensation [10], introducing distributed gratings [11], segmenting optical path into smaller sections and adding phase adjustments in between [12] etc. Compared to these schemes, QPM based on lumped dissipation is simple and universal in the sense that it is transparent to original characteristics of the nonlinear media, interacting wavelength etc., highlighting the compatibility of the scheme.

2. QPM Based on Lumped Dissipation

To illustrate the mechanism of QPM based on lumped dissipation, we start from a set of three coupled equations describing the evolution of the amplitudes along the propagation distance z in conventional single pump scenario as shown in Fig. 1(c) [13]:

$$\frac{dA_p}{dz} = i\gamma(2P - P_p)A_p + 2i\gamma A_s A_i A_p^* \exp(i\Delta\beta z), \tag{1a}$$

$$\frac{dA_s}{dz} = i\gamma(2P - P_s)A_s + i\gamma A_p A_p A_i^* \exp(-i\Delta\beta z), \tag{1b}$$

$$\frac{dA_i}{dz} = i\gamma(2P - P_i)A_i + i\gamma A_p A_p A_s^* \exp(-i\Delta\beta z), \tag{1c}$$

where subscript p, s, i represent pump, signal and idler wave, respectively. A_j represents field amplitude and $P_j = |A_j|^2$ represents power. $P = P_p + P_s + P_i$. γ is the nonlinear parameter and $\Delta\beta = \beta(\omega_s) + \beta(\omega_i) - 2\beta(\omega_p)$ is the linear phase mismatch between the propagation constants. When the pump wave is much more intense than the other waves, effective phase mismatch must be modified as $\kappa = \Delta\beta + 2\gamma P_p$, where $2\gamma P_p$ is the nonlinear momentum mismatch due to $\chi^{(3)}$ induced nonlinear refractive index. Transmission losses of all waves are not taken into account unless deliberately added. The evolution of A_s depends on the value of κ. When $|\kappa| < 2\gamma P_p$, the signal wave grows exponentially whose power can be approximated by $P_s(z) \approx K_C \exp(g_C z)P_s(0)$, where $g_C = 2g$, $K_C = (\frac{\gamma P_p}{2g})^2$, $g = \frac{1}{2}\sqrt{(2\gamma P_p)^2 - \kappa^2}$. When $|\kappa| > 2\gamma P_p$, signal evolves according to trigonometric function as $P_s(z) = K_L(z)P_s(0)$ where $K_L(z) = \frac{1}{2}\{[1 - (\frac{\kappa}{\tau})^2]\cos(\tau z) + [1 + (\frac{\kappa}{\tau})^2]\}$, $\tau = -2ig = \sqrt{\kappa^2 - 4\gamma^2 P_p^2}$. In this case, the signal wave will be amplified and attenuated periodically with τ as the period and the maximum linear gain equals to $(\kappa/\tau)^2$. $(\kappa/\tau)^2 \to 1$ when $\kappa \to \infty$, indicating

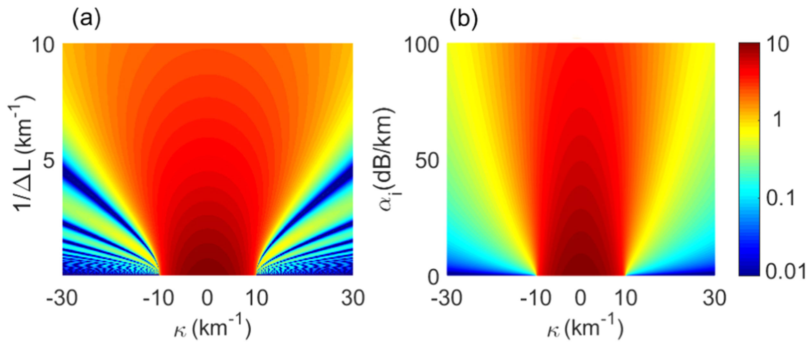

Fig. 2. Comparison of gain map with lumped or distributed dissipation as a function of phase mismatch and dissipation. (a) Gain coefficient g_L as a function of κ and ΔL with lumped losses. (b) Gain coefficient g_D as a function of κ and α_i with distributed losses. $\gamma P_p = 5\,\text{km}^{-1}$.

no amplification for large phase mismatch situation. Therefore, $|\kappa| < 2\gamma P_p$ is commonly referred to as phase matching tolerance, within which optical parametric amplifiers (OPA) can be built.

To understand the operation principle of lumped dissipation, it is better to use a set of power derivations as $-\frac{dP_p}{dz} = 2\frac{dP_s}{dz} = 2\frac{dP_i}{dz} = 4\gamma P_p\sqrt{P_s P_i}\sin\theta$ instead of Eq. (1). $A_j = \sqrt{P_j}\cos(i\phi_j)$ and $\theta = \Delta\beta z + \phi_s(z) + \phi_i(z) - 2\phi_p(z)$. It can be seen that $\sin\theta$ indicates the direction of energy flow. If the idler wave is eliminated after certain distance of propagation, the first item on the right hand side of Eq. (1c) can be dropped and Eq. (1c) could be simplified to $\frac{dA_i}{dz} = \gamma P_p\sqrt{P_i}\exp[i(-\Delta\beta z + 2\phi_p - \phi_s + \frac{\pi}{2})]$. That is, the phase of idler becomes $\varphi_i = -\Delta\beta z + 2\phi_p - \phi_s + \frac{\pi}{2}$, indicating $\theta = \pi/2$ after elimination of idler wave. Therefore, $\sin\theta$ is reset to 1 each time when filtering is applied to the idler wave. Since the OPA process starts over each time after filtering out the idler, it is easy to prove that signal wave is accumulated the same amount of gain over each section (assuming identical segmentation). Therefore, $P_s(z) = G_s(z)P_s(0)$, where $G_s(z) = K_L(L/N)^N$ and N is the number of total segments. By rewriting the total gain G_s into an exponential form, i.e. $G_s = \exp(g_L z)$, $g_L = ln(K_L(\Delta L))/\Delta L$, $\Delta L = L/N$, the gain effect of lumped dissipation can be compared with conventional OPA as well as the case of distributed losses. To be rigorous the expression is only precise when z is equal to an integer multiple of ΔL. Fig. 2(a) shows the colormap of g_L as a function of κ and ΔL, where dark blue regions correspond to the wavelengths where $g_L \approx 0$. γP_p is set to be 5 km^{-1}. According to the expression of K_L, $g_L = 0$ when $\tau\Delta L = 2n\pi$, where n is an integer. Compared to the conventional OPA case which corresponds to the line where $\Delta L \to L$, the general feature is that the effective gain region is rapidly enlarged when lumped losses are added to the system more frequently. That is, lumped dissipation indeed turns a large part of the spectrum with cosine evolution into exponential development. For the case of distributed dissipation, κ should be modified as $\kappa = \Delta\beta + 2\gamma P_p - i\alpha_i/2$ [5]. Note that all the items containing κ must be modified accordingly and the evolution of signal wave can be found as $P_s(z) \approx K_D\exp(g_D z)P_s(0)$, where $g_D = 2[Re(g) - \alpha_i/4]$ and $K_D = \frac{1}{4|g|^2}\gamma^2 {P_p}^2(\frac{g_D + \alpha_i}{g_D})$. Fig. 2(b) plots g_D as a function of κ and α_i with the same value of γP_p. After quite a few steps of derivations, $Re(g)$ can be shown to be always greater than $\alpha_i/4$. This is exactly what has been shown in Fig. 2(b), where exponential gain is achieved over the entire spectra when distributed losses are introduced, i.e. $\alpha_i > 0$.

Strong similarities can be found between the spectra of lumped and distributed cases. First, gain bandwidth is greatly improved by adding losses to the idler wave and the bandwidth increases as the total dissipation increases. Second, in both cases, the maximum gain obtained in the phase-matched region decreases as loss increases. However, such effect further improves the flatness of the gain spectra. This is highly beneficial in applications where the gain flatness other than absolute gain is the most important issue such as broadband signal processing [14]. Differences between the lumped and distributed cases are mainly the fact that there exists zero-gain point on the spectrum in lumped cases while there is not in distributed case. That is, the phase matching

TABLE 1
Evolution of Signal Power in Three Different OPAs

Situation	$P_s(z)$	Notes
Lumped losses	$\exp(g_L z)P_s(0)^*$	$\sqrt{\kappa^2 - 4\gamma^2 P_p^2}\Delta L \neq 2n\pi$
Distributed losses	$K_D \exp(g_D z)P_s(0)$	
Conventional	$K_C \exp(g_C z)P_s(0)$	$\lvert\kappa\rvert < 2\gamma P_p$

$^*z = N\Delta L$, N is an integer.

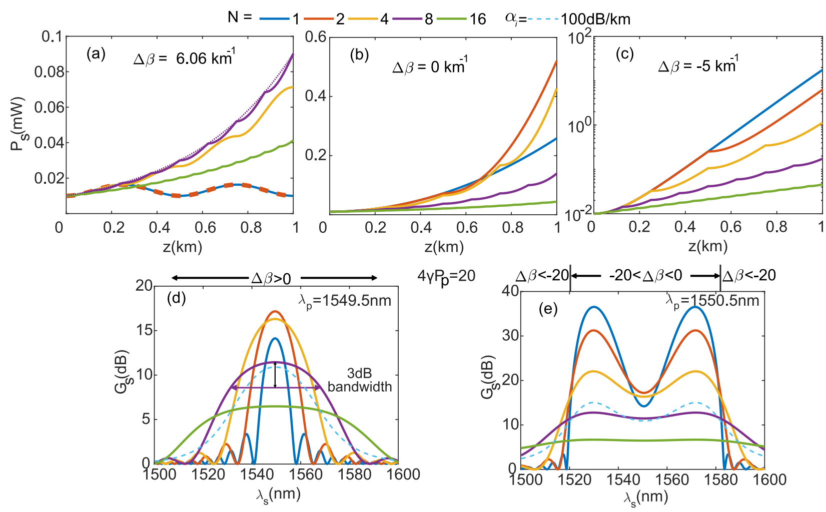

Fig. 3. Impact of dissipation on the signal evolution and gain spectra. Lumped dissipation is indicated by the number of segments N. N = 1 corresponds to the case of conventional OPA. (a–c) Evolution of the power of signal as a function of propagation distance z with lumped dissipation under the following different linear phase mismatch: (a) $\Delta\beta = 6.06\,\text{km}^{-1}$, (b) $\Delta\beta = 0\,\text{km}^{-1}$ and (c) $\Delta\beta = -5\,\text{km}^{-1}$. In (a), the purple dotted curve is simulated by analytical expression and the red line is dotted and bold to show the blue curve that coincides with it. (d, e) Gain spectra with lumped dissipation when λ_p is located in the normal (d) and anomalous dispersion region. The blue dotted curves are distributed cases with loss of idler: $\alpha_i = 100\,\text{dB/km}$. In all cases, the total length of fiber is 1 km and the zero dispersion wavelength $\lambda_0 = 1550\,\text{nm}$.

condition of $|\kappa| < 2\gamma P_p$ in the conventional OPA is relaxed into $\sqrt{\kappa^2 - 4\gamma^2 P_p^2}\Delta L \neq 2n\pi$ in the case of lumped losses but no limitations in distributed losses. However, compared to distributed losses, lumped losses are easier to be realized because it is challenge to modify the loss coefficient α_i along the entire fiber. Analytical expressions of $P_s(z)$ are summarized in Table 1.

Next we consider the impact of N on the signal evolution in lumped cases based on numerical simulations of Eq. (1). When the total length of the nonlinear media is fixed, an increase of N is equivalent to a decrease of ΔL. To keep the discussion simple while not losing the generality, uniform filtering interval and small signal gain regime is considered. The waveguide is chosen to be a highly nonlinear fiber (HNLF) whose parameters are $\gamma = 10\,\text{W}^{-1}\text{km}^{-1}$, $\beta_3 = 0.1\,\text{ps}^3\,\text{km}^{-1}$, $\beta_4 = 10^{-4}\,\text{ps}^4\text{km}^{-1}$, where β_n represents the n th-order dispersion parameters at zero dispersion wavelength ($\lambda_0 = 1550\,\text{nm}$). The total length of the HNLF is $L = 1\,\text{km}$. $P_s(0) = 0.01\,\text{mW}$ and $P_p(0) = 500\,\text{mW}$ are chosen to satisfy pump undepleted approximation. Therefore, the phase matching tolerance in this case is $|\kappa| < 2\gamma P_p = 10\,\text{km}^{-1}$ or equivalently, $-20\,\text{km}^{-1} < \Delta\beta < 0$.

The value of N impacts the total gain by changing the gain of each segment and the times of accumulation. Fig. 3(a) shows the evolution of signal power P_s along propagation distance z when $\Delta\beta = 6.06\,\text{km}^{-1} > 0$, which does not fall in the phase matching tolerance. Therefore, $P_s(z)$ varies according to trigonometric function and the average power fluctuation is very limited without lumped dissipation, i.e. $N = 1$, as shown by the blue line. The evolution of $N = 2$ (red dashed line) stays the same as $N = 1$. The reason is that according to the expression of κ, $\tau = 4\pi$ km^{-1} in this case. Since $L = 1$ km, $\Delta L = 1$ km (0.5 km) when $N = 1$ (2), leading to $\tau \Delta L = 4\pi$ (2π). Therefore, $K_L = 1$ for $N = 1, 2$. Dissipation introduced at the middle of the HNLF ($N = 2$) does not improve the gain performance because dissipation is added when the signal wave returns to its original value. When $N > 2$, idler wave is removed before signal wave gets back to $P_s(0)$. Therefore, P_s can be accumulated section by section, leading to a quasi-exponential gain as indicated by the yellow ($N = 4$), purple ($N = 8$) and green ($N = 16$) lines. The dotted purple line is calculated according to the expression shown in first line of Table 1 using $N = 8$, which coincides with the purple line when z is an integer multiples of ΔL, as expected. Next we look at the region when $\Delta\beta$ is close to 0 or -20 km^{-1} ($-4\gamma P_p$). In this case, $\tau \approx 0$ and K_L can be found to be $1 + (\gamma P_p L/N)^2$ using L'Hospital's Rule. In both cases, G_s varies non-monotonically as N increases since $G_s(z) = K_L^N$, where $K_L > 1$ and decreases with N. Fig. 3(c) shows the case when $\Delta\beta = -5$ km^{-1}, corresponding to phase-matched region. Different from Fig. 3(a) and 3(b), G_s decreases as N increases monotonically. This is because $K_L = K_C \exp(g_c L/N)$ and $G_s = K_C^N \exp(g_C L)$ in this case, where both K_C and g_c are independent of N. Therefore, G_s decreases with N if $K_C < 1$, corresponding to $|\kappa| < \sqrt{3}\gamma P_p$. It is clear $\Delta\beta = -5$ km^{-1} gives $\kappa = 5$ km^{-1}, which is smaller than $\sqrt{3}\gamma P_p = 5\sqrt{3}$ km^{-1}. By setting the pump wavelength in the normal dispersion region ($\lambda_p < \lambda_0$), Fig. 3(d) shows G_s versus λ_s when $\Delta\beta > 0$, which clearly shows the non-monotonic nature of G_s when N increases. Fig. 3(e) shows the gain spectra when λ_p is located in the anomalous dispersion region ($\lambda_p > \lambda_0$). In this case, $\Delta\beta < 0$. Therefore, part of the spectra falls in the phase matched region, corresponding to the middle section of the spectra, where monotonic decrease of G_s with N can be observed. The impact of distributed dissipation with loss of idler equal to 100 dB/km is also included in Fig. 3(d) and (e), as shown by the blue dotted curves. It can be seen that the effect of $\alpha_i = 100$ dB/km is still worse than that of N = 8, which is not easy to access considering the difficulty of introducing distributed losses. On the other hand, as will be shown later in the experimental validation, lumped dissipation offers a more systematic and practical solution.

In general, the gain increases in the non-phase-matched region while decreases in the phase-matched region as N increases. Therefore, QPM enlarges bandwidth and improves flatness of the gain spectrum. To characterize gain broadening and flattening, we define a 3 dB bandwidth as the bandwidth when the gain is reduced by 3 dB from the maximum point, as shown in Fig. 3(d) and 3(e). It is clear that the 3-dB bandwidth could be broadened greatly in the anomalous dispersion region by reducing the gain variation between the phase matched and mismatched region, as shown by the green curve in Fig. 3(e), whose 3 dB bandwidth exceeds 100 nm. We have checked the impact of the magnitude of attenuation of the idler wave per section. The criterion for the extinction ratio (ER) of the filters are chosen as a bandwidth decrease of about 10% compared to infinite ER (or 100 dB loss). No obvious differences are found between lumped dissipation with infinite large losses per section, as shown in Fig. 3, and losses greater than 25 dB per section. Numerical results shown in Fig. 3 which are calculated with Eq. (1) are also checked with full wave simulations utilizing nonlinear Schrödinger equation, showing good agreements since the requirement of undepleted pump is satisfied under given parameters.

3. Experimental Validation

According to the aforementioned theory and numerical simulations, we further carry out experiments to verify the QPM effect based on lumped dissipation using the system setup shown in Fig. 4(a). Two CW lights from tunable lasers are applied as pump and signal in OPA process. In order to suppress SBS effect, phase modulation of the pump is performed using a pseudo-random code at 10 Gbit/s. Then the signal and amplified pump enter the HNLF through a 10:90 coupler to generate OPA. It is noted that in order to ensure undepleted-pump, the signal light entering the HNLF is controlled to be as low as 0.1 mW while the pump power is about 800 mW. Two different system configurations are used for comparison. In the first configuration, three segments of 100 m HNLF with $\gamma = 10$ W^{-1}km^{-1} and $\lambda_0 = 1553.8$ nm are directly connected in series, corresponding to

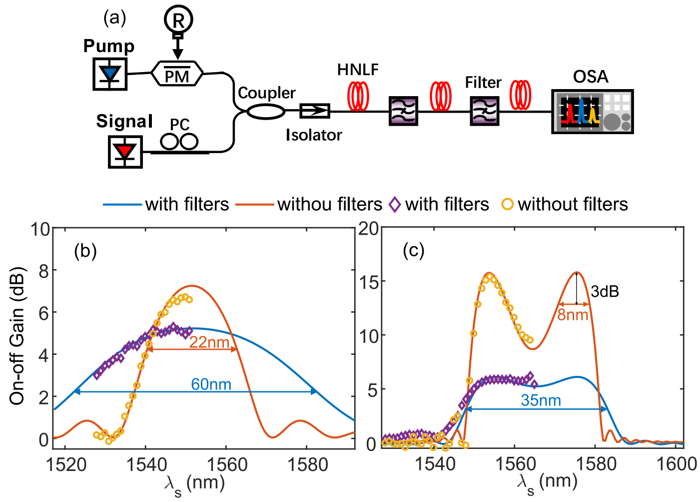

Fig. 4. Experimental validation. (a) Experimental setup to verify the quasi-phase matching (QPM) by lumped dissipation. PM: phase modulator; PC: polarization controller; R: radio frequency source; HNLF: highly nonlinear fiber; OSA: optical spectrum analyzer. (b, c) The on-off gain spectra with or without the QPM at normal (b) and anomalous dispersion region (c). The diamonds and circles are the experimental data, and solid lines are the simulation results. The red curves and yellow circles represent the cases without filters, i.e. conventional OPA. The blue curves and purple diamonds represent the cases with filters, i.e. lumped dissipation schemes.

conventional OPA case. In the second configuration, a wavelength division multiplexer with 25 dB attenuation of the idler wave is added after each segment of HNLF to achieve lumped QPM (except for the last segment), as shown in Fig. 4(a). Finally, the OPA spectra are acquired with an optical spectrum analyzer. The on-off gain can be obtained by comparing the power variation of the signal with pump power on or off. Scanning the wavelength of the signal gives the characteristics of gain spectra under this pump.

The measured on-off gain characteristics with or without the QPM are shown in Fig. 4(b, c). In the normal dispersion region ($\lambda_p = 1551.5$ nm), the gain spectra with and without filters are shown by the purple diamonds and orange circles, respectively, as shown by Fig. 4(b). Solid lines are simulations results based on solving full wave nonlinear Schrödinger equations using parameters used in the experiments. Connection losses caused by adding filters are taken into considerations. The impact of longitudinal fluctuations of dispersion of the fibers are small due to short interaction length. It is clear that when lumped dissipation is introduced to the system, 3 dB-bandwidth is broadened from 22 to 60 nm. Meanwhile, when the pump is in the anomalous dispersion region ($\lambda_p = 1565$ nm), part of the spectra falls in the phase matching tolerance. Although the maximum gain in the phase-matched region is reduced as expected, 3-dB gain bandwidth is broadened by about four times, i.e. from 8 to 35 nm as shown in Fig. 4(c). Note that the wavelengths included in only one wing of the bandwidth, either smaller or larger than the pump wavelength, can be amplified simultaneously, compared to conventional OPA. In both cases the simulation results are in good agreement with the experimental results, showing exactly the same feature as in Fig. 3(d) and Fig. 3(e).

4. Wavelength Conversion

All the above discussions we focus on the application of amplifying the signal light by attenuating the idler light. However, due to the inherent spectrum symmetry of OPA, similar mechanism will apply when dissipation is added to the signal wave for applications such wavelength conversion (WC). Instead of signal gain G_s, conversion efficiency (CE $= P_i(z)/P_s(0)$) is usually discussed in this case. With QPM, signal wave is attenuated periodically after each segment while idler wave is generated in the first segment of the fiber and amplified in latter segments. Fig. 5(a) and 5(b)

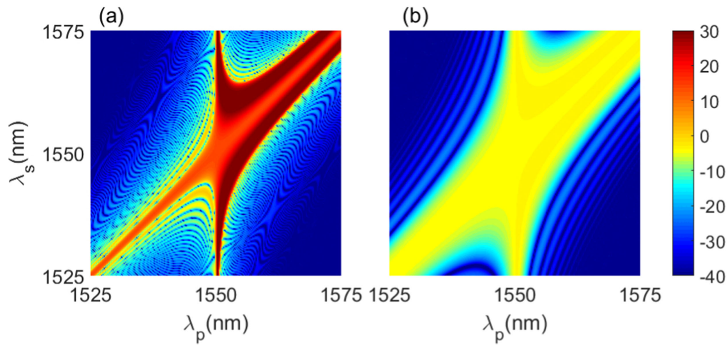

Fig. 5. Two-dimensional plot of the conversion efficiency as a function of pump and signal wavelength in the case of (a) conventional wavelength conversion and (b) lumped dissipation is introduced into signal with N = 16. The part of CE $<$ −40 dB is painted in dark blue. The simulation parameters are the same as above figures.

shows the two-dimensional plot of the CE as a function of λ_p and λ_s for no dissipation (left panel) and $N = 16$ (right panel), respectively. The simulation parameters are the same as Fig. 3. All the regions with CE < -40 dB are treated as CE $= -40$ dB to share the same dark blue color. It is clear that lumped dissipation improves the flatness of CE in wavelength conversion scenario, as expected from symmetry considerations.

5. Conclusion

In conclusion, the impact of lumped dissipation on optical parametric processes has been shown to exhibit strong similarities to that of the distributed dissipation by comparing their corresponding gain formulations. Further experimental validation is provided. While distributed losses contribute to non-hermitian phase matching, the role of lumped dissipation is to provide a simple and universal quasi-phase matching mechanism. In both dissipation scenarios, exponential gain exists over a much broader bandwidth when pump lies in the normal dispersion region while significant gain flattening is enabled when pump lies in the anomalous dispersion region. However, distributed dissipation is difficult to implement and large attenuation is usually required. As an alternative, distributed dissipation can be simply realized using a series of optical filters while the bandwidth broadening can be adjusted by changing the number of filters. Towards practical implementations, optical filters with extinction ratio greater than 25 dB are enough for the effect, which is a common feature in fiber optical communication systems. The inherent similarities revealed between lumped and distributed dissipation in this work paves an effective way to access the rich physics in nonlinear optics that are otherwise induced by distributed losses.

References

[1] T. Tanemura, Y. Ozeki, and K. Kikuchi, “Modulational instability and parametric amplification induced by loss dispersion in optical fibers,” *Phys. Rev. Lett.*, vol. 93, Oct. 2004, Art. no. 163902.
[2] R. El-Ganainy, J. I. Dadap, and R. M. Osgood, “Optical parametric amplification via non-hermitian phase matching,” *Opt. Lett.*, vol. 40, no. 21, pp. 5086–5089, 2015.
[3] J. Ma *et al.*, “Quasi-parametric amplification of chirped pulses based on a Sm^{3+}-doped yttrium calcium oxyborate crystal,” *Optica*, vol. 2, no. 11, pp. 1006–1009, Nov. 2015.
[4] A. M. Perego, S. K. Turitsyn, and K. Staliunas, “Gain through losses in nonlinear optics,” *Light: Sci. Appl.*, vol. 7, no. 1, 2018, Art. no. 43.
[5] K. Xu, H. Liu, Y. Dai, J. Wu, and J. Lin, “Synthesis of broadband and flat parametric gain by idler loss in optical fiber,” *Opt. Commun.*, vol. 285, no. 5, pp. 790–794, 2012.
[6] S. Roy, M. Santagiustina, A. Willinger, G. Eisenstein, S. Combri, and A. De Rossi, “Parametric gain and conversion efficiency in nanophotonic waveguides with dispersive propagation coefficients and loss,” *J. Lightw. Technol.*, vol. 32, no. 6, pp. 1177–1182, Mar. 2014.
[7] L. Zhang *et al.*, “Widely tunable all-fiber optical parametric oscillator based on a photonic crystal fiber pumped by a picosecond ytterbium-doped fiber laser,” *Opt. Lett.*, vol. 38, no. 22, pp. 4534–4537, Nov. 2013.

[8] H. Zhu *et al.*, “Gain optimization of one-pump fiber-optical parametric amplifier with optical band-pass filter reducing the idler wave,” *Opt. Eng.*, vol. 51, no. 9, 2012, Art. no. 095003.
[9] K. Inoue, “Arrangement of fiber pieces for a wide wavelength conversion range by fiber four-wave mixing,” *Opt. Lett.*, vol. 19, no. 16, pp. 1189–1191, Aug. 1994.
[10] M. E. Marhic, F. S. Yang, M.-C. Ho, and L. G. Kazovsky, “High-nonlinearity fiber optical parametric amplifier with periodic dispersion compensation,” *J. Lightw. Technol.*, vol. 17, no. 2, pp. 210–215, Feb. 1999.
[11] J. B. Driscoll *et al.*, “Width-modulation of Si photonic wires for quasi-phase-matching of four-wave-mixing: Experimental and theoretical demonstration,” *Opt. Exp.*, vol. 20, no. 8, pp. 9227–9242, 2012.
[12] J. Kim, O. Boyraz, J. H. Lim, and M. N. Islam, “Gain enhancement in cascaded fiber parametric amplifier with quasi-phase matching: Theory and experiment,” *J. Lightw. Technol.*, vol. 19, no. 2, p. 247, Feb. 2001.
[13] G. P. Agrawal, *Nonlinear Fiber Optics*. New York, NY, USA: Academic, 2013.
[14] M. Lillieholm, P. Guan, M. Galili, M. Møller-Kristensen, L. Grüner-Nielsen, and L. K. Oxenløwe, “Optimization and characterization of highly nonlinear fiber for broadband optical time lens applications,” *Opt. Exp.*, vol. 25, no. 11, pp. 12566–12580, 2017.